Molecular Plant Advance Access published April 5, 2012

Molecular Plant • Pages 1–10, 2012 RESEARCH ARTICLE

Quantitative Changes in Microtubule Distribution Correlate with Guard Cell Function in *Arabidopsis*

William R. Eisinger[a,b], Viktor Kirik[c], Charlotte Lewis[a], David W. Ehrhardt[b] and Winslow R. Briggs[b,1]

a Department of Biology, Santa Clara University, Santa Clara, CA 95053, USA
b Department of Plant Biology, Carnegie Institution for Science, Stanford, CA 94305, USA
c School of Biological Sciences, Illinois State University, Normal, IL 61790, USA

ABSTRACT Radially arranged cortical microtubules are a prominent feature of guard cells. We observed guard cells expressing GFP-tubulin (GFP-TUA6) with confocal microscopy and found recognizable changes in the appearance of microtubules when stomata open or close (Eisinger et al., 2012). In the present study, analysis of fluorescence distribution showed a dramatic increase in peak intensities of microtubule bundles within guard cells as stomata open. This increase was correlated with an increase in the total fluorescence that could be attributed to polymerized tubulin. Adjacent pavement cells did not show similar changes in peak intensities or integrated fluorescence when stomatal apertures changed. Imaging of RFP-tagged end binding protein 1 (EB1) and YFP-tagged α-tubulin expressed in the same cell revealed that the number of microtubules with growing ends remained constant, although the total amount of polymerized tubulin was higher in open than in closed guard cells. Taken together, these results indicate that the changes in microtubule array organization that are correlated with and required for normal guard cell function are characterized by changes in microtubule clustering or bundling.

Key words: cell differentiation/specialization; cytoskeleton; fluorescence imaging; organelle biogenesis/function; *Arabidopsis*.

INTRODUCTION

Guard cells expressing GFP-tubulin show microtubules arranged into radial arrays with respect to the stomatal aperture. These arrays are dynamic and the number of readily detectable radial-array elements declines when stomata close (Eisinger et al., 2012). Array integrity or turnover appears to affect guard cell function; oryzalin (0.1 mM) disrupts microtubule structures in guard cells and prevents light-induced stomatal opening while taxol (20 μM) stabilizes microtubule structures in guard cells and delays stomatal closure in the dark (Eisinger et al., 2012), results supporting an active role of microtubules in guard cell function. In similar experiments, Fukuda et al. (1998) also found a correlation between guard cell function and microtubule changes in the presence of inhibitors, as did Zhang et al. (2008). It should be mentioned that Yu et al. (2001) reported that oryzalin and taxol both inhibited both light-induced opening and closing in darkness and other researchers did not find a positive correlation between microtubule changes and guard cell function (Assmann and Baskin, 1998; Marcus et al., 2001). The number of growing microtubule ends and the rates of microtubule assembly, as measured by imaging of GFP-end-binding protein 1 (GFP-EB1), remain constant as detectable guard cell microtubule structures decline in number during stomatal closing (Eisinger et al., 2012). Since the assembly of microtubules remains constant, it appears that the observed loss of guard cell microtubule structures is likely caused largely by increasing microtubule instability as stomata close.

Cortical microtubules in plant cells can exist as individuals or associate with other microtubules to form bundles (Ledbetter and Porter, 1963). These bundles can be made up of parallel or anti-parallel microtubules (Shaw et al., 2003; Chan et al., 2009; Lucas et al., 2011), and have been proposed to play important roles in cell-wall biosynthesis because they form more stable guidance rails for cellulose synthesis than do the very dynamic single tubulin polymers in the cortical array (Paredez et al., 2006). The possible role of microtubule bundles in other plant cell processes remains to be determined.

[1] To whom correspondence should be addressed. E-mail briggs@stanford.edu, tel. (650) 739-4207, fax 650-325-6857.

doi: 10.1093/mp/sss033
Received 16 November 2011; accepted 25 February 2012

In this paper, we present evidence that increased clustering or bundling might account for the increases in GFP-tubulin fluorescence as guard cells open their stomata. For simplicity, we will use the term 'bundling' throughout, while remaining aware that we can not distinguish microtubules that are physically associated with each other from microtubules that are aligned with each other at a spacing below the optical resolution limit.

RESULTS

Correlation of Microtubule Signal Distribution with Stomatal Aperture

Microtubules in guard cells are known to be radially arranged and to change in appearance as the stomata open or close (Fukuda et al., 1998; Zhang et al., 2008; Eisinger et al., 2012). We therefore investigated further why microtubules appear so different in guard cells with open and closed stomata. As an initial step, we measured the distribution of fluorescence intensity in 3-D confocal-image stacks acquired from guard cells expressing GFP-tubulin A6 (GFP-TUA6) (Ueda et al., 1999). These stacks were acquired from approximately the upper half of the cell volume and were interrogated along a rectangular sample area 5 × 30 microns placed in the center of each guard cell image (Figure 1). The signal was integrated across the short axis of this measurement region using analysis tools in ImageJ and displayed as an intensity profile along the long axis of the rectangle. The solid white arrow on the upper guard cell image indicates a region of a bright linear microtubule structure; the solid black arrow on the graph shows the corresponding fluorescence peak. The dashed white arrow on the guard cell image indicates a region of very low fluorescence; the dashed black arrow on the graph shows the corresponding valley. The overall profiles show not only the approximate number of labeled structures in the defined region of a guard cell (at least eight in the upper guard cell), but also the range of fluorescent intensities among these structures.

We used the Plot Profile technique to measure hundreds of guard cells with open and closed stomata in paired sets using identical image acquisition settings on each day of acquisition. To account for changes in day-to-day instrument performance (primarily optical alignment of the excitation pathway), results were normalized for each set of daily results by dividing all values for each day by the highest measured peak in the set of open and closed cells. In Figure 2A, representative profiles of guard cells from open (six) and closed (four) stomata are plotted on the same axes, revealing an interesting pattern. Nearly all profiles from guard cells with closed stomata show a majority of profile peaks in the 20 range of relative fluorescence units, with only a few as high as 40. However, guard cells with open stomata show many peaks in the 80–90 range. Hence, guard cells from open stomata showed a shift to greater fluorescence peak intensities compared to guard cells from closed stomata. We employed the same technique to measure fluorescence intensities in pavement cells immediately adjacent to the guard cells that we analyzed. The region of the pavement cell bordering the guard cell is a smooth arc

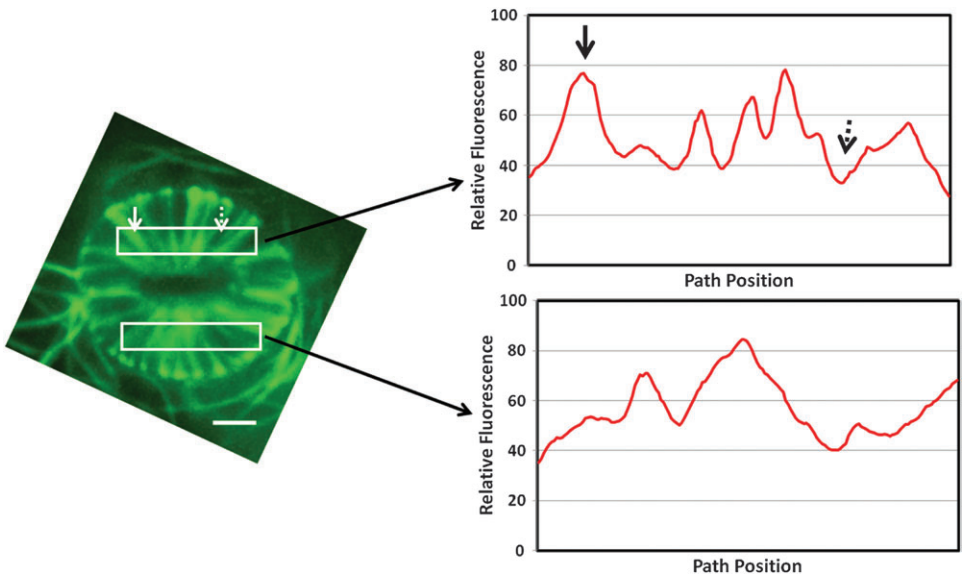

Figure 1. Measurement of GFP-Tubulin Intensity Profiles in Guard Cells.

The profiles of fluorescence signal intensity in guard cells expressing GFP-tubulin from the viral 35S promoter was measured along the axis of rectangular regions running in parallel to the axis of the stomatal aperture (rectangular boxes in image). These 5 × 30-micron regions were scanned left to right and the measured intensities plotted as profiles. The solid white arrow indicates a region of bright fluorescence and the solid black arrow on upper line graph shows the corresponding fluorescence-intensity peak. The dashed white arrow on the image indicates an area of low fluorescence intensity and the dashed black arrow on the upper line graph shows the corresponding valley. Bar = 10 microns.

and does not the show complicated pattern of lobes and necks that characterizes most pavement cells. We did our analyses of pavement cells in the region of the smooth arc to avoid the complicated topology of the lobe/neck areas. We see far less difference in the distribution of fluorescence peak intensities between pavement cells adjacent to guard cell with open (red lines) or closed (black lines) stomata (Figure 2B). Additional profiles from similar experiments but with YFP-TUA5-labeled plants can be seen in Supplemental Figure 1.

To determine whether the integrated GFP-tubulin signal is different at the cell cortex in open and closed guard cells, we integrated the signal (minus background, see 'Methods') along each profile for 73 open and 67 closed guard cells, acquired in paired sets on 15 different days and subjected these data to Analysis of Variance (ANOVA) using day of experiment and stomatal aperture as the independent variables and the integrated signal as the dependent variable. Stomatal aperture had a very significant effect on the integrated signal for both raw data and data normalized to mean signal in the open state on the day of acquisition ($P < 0.001$) (Supplemental Figure 2). The normalized signal in the closed state was 44% lower on average than that in the open state, indicating that the quantity of GFP-tubulin in the measured cell volume was significantly reduced in the closed state as compared to the open state.

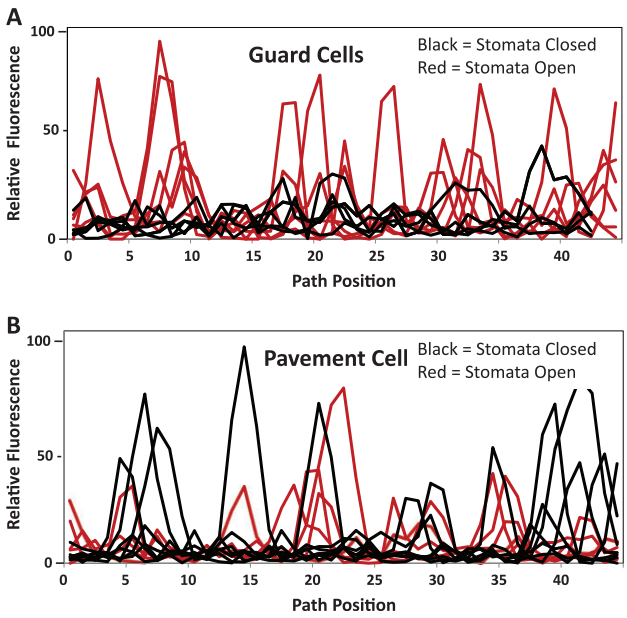

Figure 2. GFP-Tubulin Peak Intensities Are Higher in Guard Cells with Open Stomata.

(A) The intensity profiles from guard cells with open stomata (red lines, six profiles shown) show fluorescence peak intensities far higher than those of guard cells with closed stomata (black lines, four profiles shown).

(B) Adjacent pavement cells show little change in fluorescence peak intensities whether adjacent guard cells have open (red lines, six plots shown) or closed stomata (black lines, four plots shown). Plots created as illustrated in Figure 1.

Progressive Changes in Microtubule Fluorescence during Stomatal Closure

As guard cells close their stomata in darkness, there is a corresponding decrease in fluorescence peak intensities (Figure 3, left side). In the top panel, we present six profile plots of guard cells from open stomata (0 min in darkness) with dramatic peaks and valleys. Mounted pieces of leaf tissue were placed in darkness for a total of 40 min and images of individual stomata were obtained at 10-min intervals. Fewer bright peaks were seen after 10 min in darkness as stomatal aperture decreased by about 10%. With increased time in darkness, we observed a simultaneous decrease in fluorescence peak intensities and stomatal aperture. The fluorescence-intensity profiles of adjacent pavement cells decreased less dramatically in darkness (Figure 3, right side). To provide a different perspective, we present the same data as heat maps (Supplemental Figure 3). Pavement cells show fluorescence peak intensities above 50 units throughout the dark time course, indicating that this response is specific to guard cells and is not due to a physical effect of repeated imaging such as photobleaching.

Comparing the Tubulin Signal to the EB1 Signal

To investigate the relationship between changes in GFP-tubulin fluorescence peak intensity and microtubule assembly simultaneously in individual guard cells, we observed leaves from plants expressing both RFP-EB1, a marker of growing microtubule ends, and YFP-tubulin (TUA5) (Figure 4). Previous

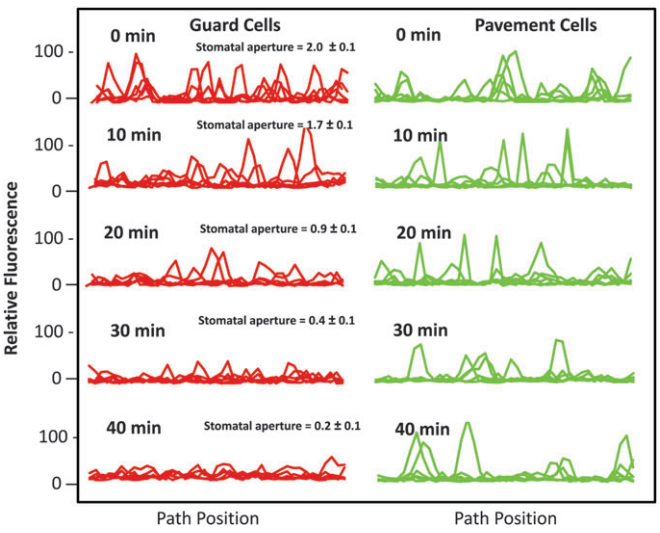

Figure 3. GFP-Tubulin Signal Profiles Show Progressive Changes during Stomatal Closure.

When placed in darkness, guard cells with open stoma show a progressive loss in fluorescence peak intensities and a decrease in stomatal aperture (left side, red lines). Plots of adjacent pavement cells showed less change in fluorescence peak intensities (right side, green lines). Six guard cell and five pavement cell plots shown (right side, green lines).

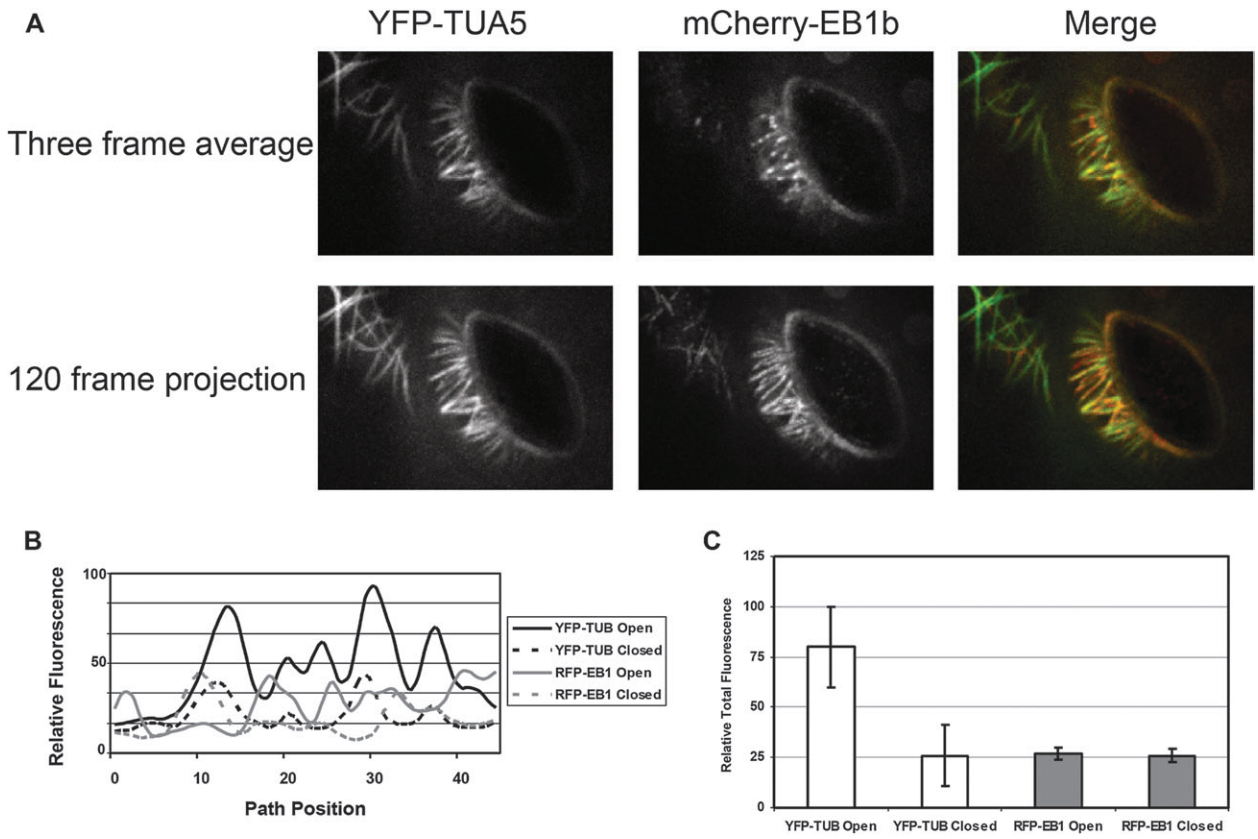

Figure 4. New Assembly of Microtubules, as Assessed by mCherryEB1, Is Similar in Guard Cells from Open and Closed Stomata.

(A) Images of closed guard cells co-expressing YFP-TUA5 and the plus-end-associated protein mCherry-EB1 (top row). Brightest point projection of a 120-frame time series (240 seconds) shows tracks of EB1 signal as microtubules assemble (bottom row).

(B) Representative profile plots from the time projected images from guard cells from plants expressing both labels. Consistent with experiments using YFP-TUA5 alone, YFP-TUA5 peak fluorescence intensity is greater in guard cells when stomata are open (solid black lines) than when stomata are closed (dashed black lines). RFP-EB1 peak fluorescence (solid and dashed gray lines), however, remains relatively unchanged with opening.

(C) Quantitation of integrated fluorescence from profile plots. Guard cells from plants expressing both RFP-EB1 and YFP-tubulin showed significant increases in total YFP-tubulin fluorescence when stomata open (white bars), but no change in signal arising from the projected trajectories of the growing plus ends labeled with RFP-EB1 (gray bars). Error bars are standard deviations. n = 20. Scale bar = 10 microns.

studies using cells expressing GFP-EB1 alone (Eisinger et al., 2012) showed that both the number of growing ends and the rate of plus-end growth were similar in open and closed guard cells, so the projected images are an indication of the amount and position of new microtubule growth over the imaged interval. An important question, though, was whether expression of GFP-EB1might alter microtubule stability in guard cells in a manner that would affect interpretation of the experiment. For plants used in this series of experiments, YFP-tubulin expression and RFP-EB1 expression were driven by 35S promoters. Presumably due to co-suppression, some guard cell pairs expressed both labels, some showed YFP only, and others showed RFP only within a given leaf. For our analyses, we selected only guard cells that expressed both labels strongly.

Images of guard cell pairs expressing both markers are shown in Figure 4A; the green channel (YFP-TUA5) shows radially arranged microtubule structures. The red channel shows mCherry-EB1b localized to the growing ends of microtubules as short 'comets'. One hundred and twenty-frame time projections of EB1 'comets' appear as linear structures that largely colocalize with YFP-TUA5 microtubule structures (merge). The distribution of fluorescence intensities and the integrated intensities of both channels were analyzed as described above for the cells expressing GFP-tubulin alone. Representative profile plots from plants expressing both labels are shown in Figure 4B. There was no observed significant difference in the peak profiles or integrated intensities for RFP-EB1 between guard cells with open and closed stomata (Figure 4B and 4C), consistent with our previous observation that the number and velocities of EB1 comets were similar in both states. By contrast, the YFP profiles (tubulin) and integrated intensities did show pronounced differences in the open and closed states (Figure 4B and 4C), and in a similar fashion to that observed in cells expressing a tubulin marker alone (Figures 2 and Supplemental Figure 2). These results confirmed

that microtubule assembly, as assayed by EB1 localization and dynamics, is similar in the open and closed state, although the distribution of labeled microtubules and the integrated YFP-tubulin signal changes.

Refinement of Imaging and Analysis of Microtubule Distribution

While the above experiments and measurements had shown robust differences between guard cells with open and closed stomata, we had also observed during the course of these experiments that the brightness and sharpness of the images were often degraded due to uncorrected spherical aberration. In addition, we also had obtained images from only the upper half of the cell volume in these experiments, caused in large part by the same issue of degraded image quality owing to increased spherical aberration with greater focal depth. To refine our technique and to obtain information from the whole-cell volume, we employed a glycerol immersion objective with a correction collar and performed a correction of each imaged pair of guard cells to optimize image quality. In addition, we collected focal volumes at a higher pixel sampling frequency by employing a 1.6× optivar and we sampled the *z*-axis at approximately 3× the optical resolution. Improved measurements were made from these enhanced volumes by isolating microtubule signal along three rather than two dimensions to reduce signal variance from the cell background. This was accomplished by drawing curved transects down the middle of the longitudinal axis of each cell to sample most microtubule structures on an orthogonal axis (Figure 5A, from a guard cell from an open stoma), then using these transects to re-slice the volume along the *z*-axis to create a 2-D image parallel to the optical axis (Figure 5B). The fluorescence intensities of the cross-sectional images of cortical microtubules were then quantified as previously, by using the 'Plot Profile' feature of ImageJ (Figure 5C). This technique greatly improved our ability to identify individual microtubule structures, detecting more discrete structures than had previously been possible (Figure 1; see Eisinger et al., 2012).

The first observation made with these datasets was that there was no evidence for an unexpected redistribution of the microtubule array along the *z*-axis of the cell that could explain the measured changes in signal intensity (Supplemental Figure 4). Next, the enhanced datasets were used for analysis of shifts in the fluorescence peak distribution. Ranking of

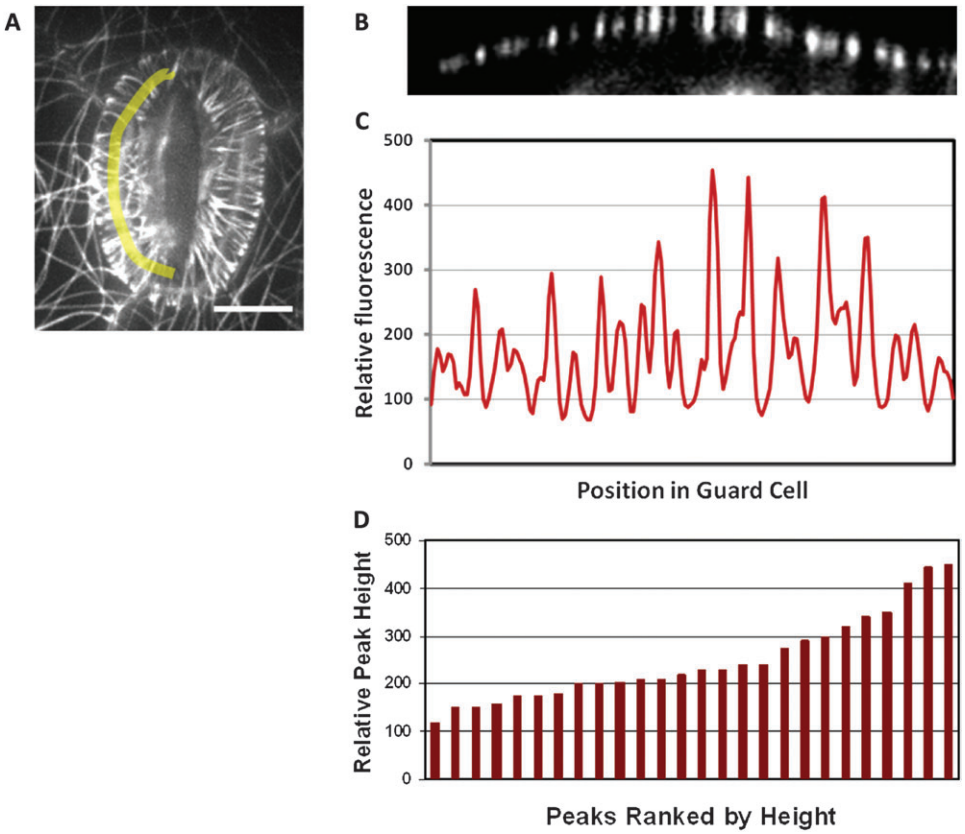

Figure 5. Enhanced Measurement of GFP-Signal Intensity Distribution Using 3-D Image Volumes.

Higher-resolution datasets were acquired (see 'Results') and the signal associated with cortical microtubules was isolated better by re-slicing the image volume using a curved transect along the guard cell axis **(A)** then creating intensity profiles from the resulting *x–z* images **(B)**. This method created more distinct intensity peaks **(C)** that were then measured and ranked according to peak intensity value **(D)**. Bar = 10 microns.

the measured peaks (Figure 5D) revealed regions of plateaus (little change in peak height) and regions of transition (changes in peak height). We propose that these graphic patterns reflect discreet levels of microtubule clustering and perhaps physical bundling. For example, in this illustration, peak heights near 100 units might correspond to single microtubules; heights near 200 units might represent microtubules in pairs; heights near 300 units might be bundles of three microtubules, etc. Supplemental Figure 4 shows graphs of ranked peak heights for six representative guard cell pairs from open stomata. Although there is variation among the profiles, all show the general pattern of transitions and plateaus shown in Figure 5D and are consistent with stepwise differences in microtubule clustering or bundling state.

Measurements of fluorescence peak distribution made with the 3-D technique and visualized as ranked peaks were consistent with our previous 2-D measurements. Guard cells from leaves treated with continuous light (Figure 6A, red bars) showed more variation and greater fluorescence peak heights (putative microtubule bundling) than these same guard cells kept in the dark overnight (Figure 6A, black bars). Moreover, when these same guard cells held in the dark were exposed to white light for 1 h (Figure 6A, blue bars), peak heights and variability increased dramatically, approaching levels seen with continuous light (red bars). In another experimental series (Figure 6B), 0.1 M KCl treatment, which prevented dark-induced stomatal closure, maintained fluorescence peak heights and stepwise variability (microtubule bundling) after 40 min in darkness.

Finally, we examined progressive changes in bundling state using the 3-D technique. Guard cells were placed in darkness and imaged at 10-min intervals for a total of 40 min (Figure 7). Consistent with previous results, we saw a progressive shift to lower peak height and less variability. By 40 min (black line), the overall graph is largely flat, with no values above 85 units. In order to identify the boundaries of clusters of microtubules with the same order of bundling or clustering status more easily, we mathematically amplified the transitions between plateaus. The first derivative of peak height (change in height between each peak and its next higher neighbor) was calculated for the initial ($T = 0$) and 40-min ($T = 40$) time points and plotted (Figure 7, Graph B). Possible transitions between one state of order or bundling to the next for open stomata appear as peaks in this graph; clusters of microtubules at the same order or bundling state result in a horizontal flat line. The first transition (1) likely corresponding to a step from single to double microtubules; the next (2) might be doubles to triples, etc. Consistently with the hypothesis that a positive correlation exists between microtubule bundling or clustering and guard cell function, longer periods in darkness ($T = 40$) resulted in damping of transition peaks, especially for what would correspond to higher-order bundling.

Enhanced imaging of cortical microtubules now allowed us to address the question: is the observed increase in microtubule structures as stomata open the consequence of detecting greater numbers of microtubule bundles, which would be

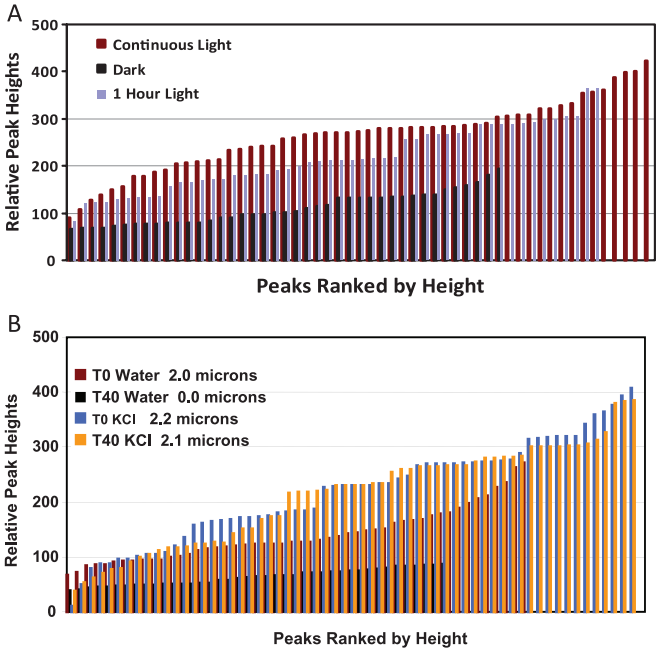

Figure 6. The Distribution of GFP-Tubulin Peak Intensities from Enhanced Datasets Correlate with Guard Cell Open/Closed State.

(A) Guard cells expressing GFP-tubulin were analyzed for microtubule-profile peak fluorescence and peaks were ranked by height as described in Figure 5. Guard cells exposed to continuous light (red bars) show greater peak height and variability among peak heights (evidence for putative increased ordering and bundling of microtubules) than those of guard cells kept in the dark (black bars). If plants from the dark were exposed to white light (100 μmol photons m^{-2} s^{-1}) for 1 h, peak heights increased, as did variability among peak heights (blue bars). The results are shown for a single guard cell used for all three measurements. We analyzed 20 guard cell pairs and results shown are representative of our findings.

(B) Guard cells treated with 0.1 M KCl (compare light blue, T0, and rose, T40, bars) did not close their stomata after 40 min of darkness and retained fluorescent peak heights and variability (microtubules remained ordered and bundled). Equivalent guard cells treated with water (compare red bars, T0, and black, T40, bars) closed their stomata in darkness and fluorescent peak heights and variability declined. The results are shown for a single guard cell used for all four measurements. This experiment was repeated 10 times; results shown are representative.

bright and easy to detect even with suboptimal imaging, or is there really a dramatic increase in the number of discreet microtubule structures, including single and thus less well-labeled microtubules (see Figure 1 in Eisinger et al., 2012)? In both of these experiments, the scan was taken over the entire length of an individual guard cell and hence presumably captured a very high percentage of the structures present. There is a somewhat larger number of structures when the stomata are open than when they are closed, shown in both figures, but nothing like the threefold increase in resolvable structures reported in Eisinger et al. (2012). Hence, on stomatal opening, the structures primarily become brighter to the point at which they were detected in previous studies, and there is only a small increase in the total number of detectable structures.

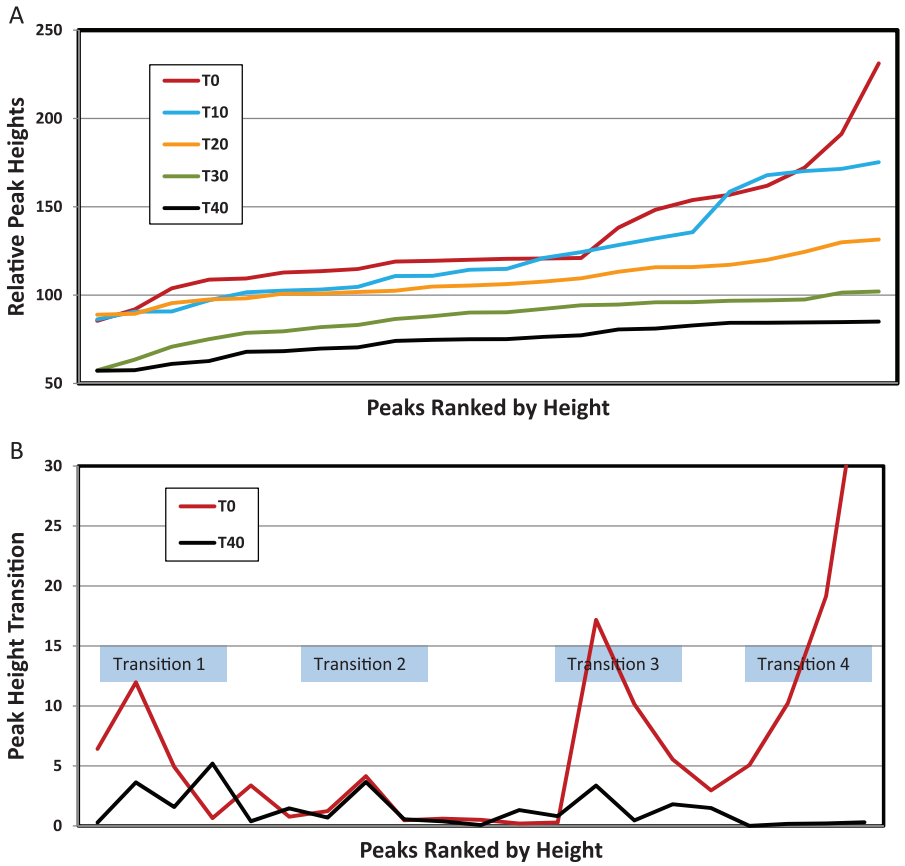

Figure 7. Guard Cells Held in Darkness Showed a Progressive Decline in Fluorescent Peak Heights and Variability.

For clarity, the ordered peak-height data are presented as line graphs **(A)**. When stomata are open (T0, red line), peak heights are variable and range to values over 200 relative units. However, with time in darkness, variability and maximum peak heights decline dramatically. For example, after 40 min in dark (T40, black line), all peak heights fall within the 55–80 range. First, derivative analysis **(B)** was used to identify transitions in fluorescent peak heights for T0 and T40. The transitional peaks represent boundaries between groups of microtubules with the same order or bundling status. For T0, there are four such peaks. These transition peaks decreased dramatically in magnitude with time in darkness as guard cell microtubules become less ordered and bundled when stomata close (compare T0, red line, and T40, black line).

DISCUSSION

Guard cells are structurally and functionally different from other epidermal cells. Radially arranged microtubules characterize guard cells and play a key role in their development. Dynamic changes visualized in confocal images of GFP-tubulin in guard cells reflect stomatal aperture closely and guard cell microtubules are uniquely sensitive to environmental factors that regulate guard cell function. We previously determined from GFP-tubulin fluorescence that both the number of detected radial elements of the cortical microtubule array and the total fluorescence signal are higher in guard cells from open stomata than those from closed stomata (Figure 6 and Eisinger et al., 2012). However, our studies with the microtubule assembly protein (EB1) indicate that assembly per se is independent of guard cell function (Eisinger et al., 2012 and this study). We hypothesized that decline in guard cell microtubules and total fluorescence as stomata close is the result of increased rates of disassembly and tubulin degradation.

A parallel issue that arises from the present study is the role of microtubule clustering or bundling in guard cell function. Quantitative fluorescence peak-height analyses show dramatic shifts in signal intensity of resolved radial microtubule structures between guard cells of open and closed stomata (Figure 2). Increased assembly into bundles as stomata open is a logical explanation for this change in distribution. Taken together, these data suggest that, in open guard cells, both the total amount of assembled tubulin and the degree of bundling are higher than in closed guard cells. We hypothesize that the overall increase in fluorescence reflects an increase in the steady-state level of total GFP-tubulin as guard cells swell, and thus also a decrease upon closing. In support of this hypothesis, Fukuda et al. (2000) reported that cyclohexamide inhibited stomatal opening in the morning.

Lahav et al. (2004) observed more order among microtubules of guard cells from open than from closed stomata both in *Commelina communis* (immunofluorescence) and *Arabidopsis thaliana* (GFP-tubulin) than in closed. From these and

our own observations, we propose that the dramatic changes in highly fluorescent structures when guard cells expressing GFP-tubulin swell or shrink in response to hormonal or environmental signals (Figures 2 and 3) can be attributed to (1) a change in assembled tubulin overall, accompanied by an increase in the steady-state level of tubulin and (2) to a change in microtubule bundling.

There are many variables associated with confocal microscopy and use of fluorescent protein markers that can make comparisons between different samples challenging. Our YFP-tubulin/RFP-EB1 double-label experiments provided a unique opportunity to monitor both microtubules and microtubule assembly simultaneously in the same cell, hence avoiding that challenge. Results from these experiments reinforced data from our experiments using single labels, and served as an important control for the possibility that expression of RFP-EB1 might interfere with microtubule assembly or stability. Guard cells with open stomata had more microtubule fluorescence and brighter peaks of tubulin fluorescence than guard cells with closed stomata (Figure 4B). EB1 signal did not change with stomatal opening in the same cells. Adjacent pavement cells did not show measurable differences in tubulin fluorescence, peak brightness, or assembly activity whether guard cell stomata were open or closed.

Cortical microtubules are well known to interact with one another to form bundles (Shaw et al., 2003; Dixit and Cyr, 2004; Barton et al., 2008). The microtubule-associated protein-65 (MAP65) family of proteins can bundle microtubules *in vitro* and are associated with bundled microtubules *in vivo* (Smertenko et al., 2004), but genetic studies indicate that MAP65 likely does not act as the primary bundling factor for cortical microtubules *in vivo* (Lucas et al., 2011). We were unsuccessful in our efforts to visualize MAP65-GFP, as the signal in available transgenics was too weak in guard cells. While our studies are limited by optical resolution, and we can not distinguish formally between bundling and some other form of microtubule association, we feel that the most parsimonious explanation for the increased signal in radial elements of the cortical array observed when guard cells open their stomata is increased microtubule bundling. When we sorted the peaks by height, we see a clear pattern of plateaus and transitions that are suggestive of progressive bundling (Figure 5). Not all guard cells exactly mirror this pattern, but representative guard cells with open stomata show patterns of progressive transitions and plateaus (Supplemental Figure 4).

When we measured changes in the peak-height pattern in response to closing or opening signals, we found a strong correlation between peak-height pattern (bundling) and guard cell function. Stomatal closure in darkness resulted in uniformly lower peak heights and less variation among peak heights consistent with decreased bundling (Figure 6A). Subsequent illumination increased peak heights and variation among peak heights, consistently with increased bundling. Treatment with KCl (0.1 M) delayed dark-induced stomatal closure and any decreased peak height (bundling) (Figure 6B). Together with the experiments on oryzalin-induced microtubule disassembly and taxol-mediated stabilization (Fukuda et al., 1998; Zhang et al., 2008; Eisinger et al., 2012), we view the KCl results as further evidence for a causal relationship between microtubule ordering and guard cell function.

The results obtained with this technique stand somewhat in contrast to those shown in the companion paper (Eisinger et al., 2012). There, we observed that the number of detectable microtubule structure in guard cells tripled as stomata opened. With the better-resolved images in the present study, it appears that the number of detectable structures in guard cells from closed versus open stomata is less important than their clustering or bundling status in accounting for the fluorescence changes.

Left unresolved is the apparent paradox that there appear to be real changes in the signal from polymerized tubulin at the cell cortex as indicated by fluorescence changes in guard cells on opening and closing but no changes in the number of growing ends or the velocity of microtubule growth. One possible scenario is that microtubules are shorter on average in the closed state than in the open due to an increased catastrophe rate at the growing ends or increased loss from minus ends (which are not labeled by RFP-EB1). A more complex scenario is that there may be two populations of microtubules, with some microtubules becoming stabilized and losing their EB1 decorations as guard cells open. To maintain the number of growing ends, initiation of new microtubules would need to keep pace with the rate of stabilization. At present, we lack information allowing us to distinguish between these two possibilities.

A time course for closure in darkness showed a progressive decline in bundling (peak height) as stomata closed (Figure 8A). To distinguish boundaries between groupings of microtubules of the same bundling status, we calculated the first derivative of peak height plotted by rank order of height (Figure 8B). This technique amplifies the transition zones that separate groupings of variously ordered microtubules. As predicted, during stomatal closure, these transitions decline in magnitude in regions of the graph where one would predict higher-order bundling. These three studies—steps and plateaus in ranked peak fluorescence in guard cells from open stomata, their persistence in the presence of KCl, and systematic changes in steps and plateaus on stomatal opening and closing—provide evidence that microtubule bundling may account for the observed changes in microtubule peak fluorescence.

How microtubule bundling and MAPs are related to guard cell function remains an open question. Cellulose synthase has recently been shown to be targeted to specific locations at the plasma membrane by cortical microtubules (Guttierrez et al., 2009). It is not known whether other protein traffic may also be targeted by cortical microtubules, but an elevation in microtubule bundling may increase the stability of the array for targeting proteins within the guard cell.

Phototropins are the photoreceptors for blue light-induced stomatal opening (Kinoshita et al., 2001). Tseng et al. (2012) report that association of a 14–3–3-λ protein

with phosphorylated PHOT2 is required for the signal transduction pathway that leads to PHOT2-mediated, blue light-induced stomatal opening. Where might microtubules lie on this pathway? Working with microtubule-impacting drugs, Yu et al. (2001), Zhang et al. (2008), and Eisinger et al. (2012) all showed a role for intact microtubules for stomatal opening and that stabilized microtubules prevented closure. Lahav et al. (2004) reported that treating guard cells with fusicoccin (2 μM), which stimulate proton pumping, resulted in stomatal opening without changes in microtubule order or number. Based on these results, they concluded that microtubules operate upstream in the stomatal opening signal-transduction pathway. While many details remain to be determined, the blue light-induced signal-transduction pathway for stomatal opening must begin with phototropin phosphorylation and 14–3–3 λ protein binding (Kinoshita and Shimazaki, 2002), involve microtubule stabilization and bundling and end with activation of plasma membrane ATPases and ion channels. We envision that phototropin signaling at the cell membrane, possibly acting in a complex with ATPase and ion-channel downstream targets, could promote microtubule stabilization through regulation of MAPs that govern microtubule stability, and, in turn, cortical microtubules would then contribute to stabilization and activity of these signaling complexes at the membrane and, ultimately, stomatal opening. Future studies will be needed to test this model.

METHODS

Plant Materials and Growth Conditions

Arabidopsis plants were greenhouse-grown relying on natural light supplemented with artificial lights (75 μmol m^{-2} s^{-1}) to ensure a minimum of a 16-h photoperiod. Temperature was modulated using heaters and evaporational cooling systems to approximately 22°C day and 20°C night.

Arabidopsis Expressing Fluorescent Proteins

Arabidopsis thaliana tubulin was visualized using either 35S::GFP-TUA6/pBS (Col-0 background) supplied by Takashi Hashimoto, Nara Institute of Science and Technology, Nara, Japan, or YFP-TUA5 (Debolt et al., 2007). To create the Cherry-EB1 construct, we replaced the *GFP* gene for the mCherry in the pMDC43 (Curtis and Grossniklaus, 2003) and introduced the AtEB1b cDNA (AT5G62500) using Gateway cloning (Invitrogen). The construct was transformed into *A. thaliana* plants expressing the YFP-TUA5 microtubule marker.

Microscopy

Images were acquired with either a Leica DM IRE2 inverted fluorescence microscope equipped with a Leica 63×, n.a. = 1.3, glycerin immersion objective lens, a Yokogawa CSU-10 spinning disk confocal head, and a Roper QuantEM camera as described (Paradez et al., 2006), or with a Leica DM6000 inverted microscope, a Leica 63×, n.a. = 1.3, glycerin immersion objective lens, a Yokogawa CSU-X spinning disk confocal head and a Roper Evolve camera. On the latter instrument, excitation was provided by a 491 solid-state laser or a 561 solid-state laser (both Cobolt, Solna, Sweden). Slidebook software was used for acquisition on both instruments (Intelligent Imaging Innovations, Denver, CO).

Measuring Stomatal Aperture

Small leaf fragments were prepared from *Arabidopsis* leaves, put onto slides as wet mounts, and stomata imaged with a light microscope. Stomatal apertures were quantified using the measurement tools in ImageJ software (Wayne Rasband, NIH). For KCl treatments, leaf fragments were prepared as wet mounts using 0.1 M KCl instead of dionized water.

Quantifying GFP-Tubulin Fluorescence

In initial studies, a rectangular template was placed over a z-projected image of a guard cell (see Figure 2). The fluorescence intensities scanned along the long axis of the rectangle were measured using the Plot Profile feature of ImageJ. For a given experimental series, the highest fluorescence peak was assigned a value of 100. All other data points within that series were normalized to that value. Background fluorescence was measured for an equivalent rectangular region immediately adjacent to the region sampled for microtubule fluorescence. These background values were subtracted from the microtubule fluorescence values.

In later studies, Z-stacks of guard cell images were assembled and an eight-pixel segmented line was drawn along the center of each guard cell (see Figure 5A). The re-slice feature of ImageJ was then used to generate the microtubule profile (Figure 5B). This profile was scanned using Plot Profile to generate a graph of peak intensity versus position along the microtubule profile (Figure 5C). Peak heights were measured and ranked by height. These data were normalized as described above and graphed (Figure 5D), with lowest heights to the left and greatest heights on the right. To determine background fluorescence, an equivalent eight-pixel-wide line was drawn in the stomatal aperture parallel to the line used to measure microtubule fluorescence. These background values were subtracted from the microtubule fluorescence values.

SUPPLEMENTARY DATA

Supplementary Data are available at *Molecular Plant Online.*

FUNDING

This work was supported by NSF Grant 0843617 to W.R.B. and funds from the Carnegie Institution for Science. The authors are grateful for this support.

ACKNOWLEDGMENTS

We wish to thank Ryan Gutierrez (Carnegie Institution for Science, Department of Plant Biology) for assistance with the double-label experiments. No conflict of interest declared.

REFERENCES

Assmann, S.M., and Baskin, T.I. (1998). The function of guard cells does not require an intact array of cortical microtubules. J. Exp. Bot. **49,** 163–170.

Barton, D.A., Vantard, M., and Overall, R.L. (2008). Analysis of cortical arrays from *Tradescantia virginiana* at high resolution reveals discrete microtubule subpopulations and demonstrates that confocal images of arrays can be misleading. Plant Cell. **20,** 982–994.

Chan, J., Sambade, J.A., Calder, G., and Lloyd, C. (2009). *Arabidopsis* cortical microtubules are initiated along, as well as branching from, existing microtubules. Plant Cell. **21,** 2298–2306.

Curtis, M.D., and Grossniklaus, U. (2003). A Gateway cloning vector set for high-throughput functional analysis of genes in planta. Plant Physiol. **133,** 462–469.

Debolt, S., Gutierrez, R., Ehrhardt, D.W., Melo, C.V., Ross, L., Cutler, S.R., Somerville, C., and Bonetta, D. (2007). Morlin, an inhibitor of cortical microtubule dynamics and cellulose synthase movement. Proc. Natl Acad. Sci. U S A. **104,** 5854–5859.

Dixit, R., and Cyr, R. (2004). Encounters between dynamic cortical microtubules promote ordering of the cortical array through angle-dependent modifications of microtubule behavior. Plant Cell. **16,** 3274–3284.

Eisinger, W., Ehrhardt, D., and Briggs, W.R. (2012). Microtubules are essential for guard cell function in Vicia and *Arabidopsis*. Mol. Plant. **5,** in press.

Fukuda, M., Hasezawa, S., Asai, N., Nakajima, N., and Kondo, N. (1998). Dynamic organization of microtubules in guard cells of *Vicia faba* L. with diurnal cycle. Plant Cell Physiol. **39,** 80–86.

Fukuda, M., Hasezawa, S., Nakajima, N., and Kondo, N. (2000). Changes in tubulin protein expression in guard cells of *Vicia faba* L. accompanied with dynamic organization of microtubules during the diurnal cycle. Plant Cell Physiol. **41,** 600–607.

Guttierrez, R., Lindeboom, J.J., Paradez, A.R., Emons, A.M.C., and Ehrhardt, D.W. (2009). Arabidopsis cortical microtubules position cellulase synthase delivery to the plasma membrane and interact with cellulose synthase trafficking compartments. Nature Cell Biol. **11,** 797–806.

Kinoshita, T., and Shimazaki, K. (2002). Biochemical evidence for the requirement of 14–3–3 protein binding in activation of the guard-cell plasma membrane H^+-ATPase. Plant Cell Physiol. **43,** 1359–1365.

Kinoshita, T., Doi, M., Suetsugu, N., Kagawa, T., Wada, M., and Shimazaki, K. (2001). PHOT1 and PHOT2 mediate blue light regulation of stomatal opening. Nature. **414,** 656–660.

Lahav, M., Abu-Abied, M., Belausov, E., Schwartz, A., and Sadot, E. (2004). Microtubules of guard cells are light sensitive. Plant Cell Physiol. **45,** 573–582.

Ledbetter, M.C., and Porter, K.R. (1963). A 'microtubule' in plant cell fine structure. J. Cell Biol. **19,** 239–250.

Lucas, J.R., Courtney, S., Hassfurder, M., Dhingra, S., Bryant, A., and Shaw, S.L. (2011). Microtubule-associated proteins MAP65-1 and MAP65-2 positively regulate axial cell growth in etiolated *Arabidopsis* hypocotyls. Plant Cell. **23,** 1889–1903.

Marcus, A.I., Moore, R.C., and Cyr, R.J. (2001). The role of microtubules in guard cell function. Plant Physiol. **125,** 387–395.

Paredez, A., Wright, A., and Ehrhardt, D.W. (2006). Microtubule cortical array organization and plant cell morphogenesis. Curr. Opin. Plant Biol. **9,** 571–578.

Shaw, S.L., Kamyar, R., and Ehrhardt, D.W. (2003). Sustained microtubule treadmilling in *Arabidopsis* cortical arrays. Science. **300,** 1715–1718.

Smertenko, A.P., Hsin-Yu Chang, H.-Y., Wagner, V., Kaloriti, D., Fenyk, S., Sonobe, S., Lloyd, C., Hauser, M.-T., and Husseya, P.J. (2004). The *Arabidopsis* microtubule-associated protein AtMAP65-1: molecular analysis of its microtubule bundling activity. Plant Cell. **16,** 2035–2047.

Tseng, T.-S., Whippo, C., Hangarter, R.P., and Briggs, W.R. (2012). The role of a 14–3–3 protein in stomatal opening mediated by PHOT2 in *Arabidopsis*. Plant Cell. doi: 10.1105/tpc.111.092130. DC1.html.

Ueda, K., Matsuyama, T., and Hashimoto, T. (1999). Visualization of microtubules in living cells of transgenic *Arabidopsis thaliana*. Protoplasma. **206,** 201–206.

Yu, R., Huang, R.-F., Wang, X.-C., and Yuan, M. (2001). Microtubule dynamics are involved in stomatal movement of *Vicia faba* L. Plant Cell Physiol. Protoplasma. **216,** 113–118.

Zhang, Y.-M., Wu, Z.-Y., Wang, X.-C., and Rong, Y.U. (2008). Rearrangements of microtubule cytoskeleton in stomatal closure of *Arabidopsis* induced by nitric oxide. Chinese Sci. Bull. **53,** 848–852.